PHYSICAL REVIEW E VOLUME 57, NUMBER 4 APRIL 1998

Critical behavior at the nematic to lamellar phase transitions: A synchrotron x-ray scattering study

S. T. Shin,[1] J. D. Brock,[2] Mark Sutton,[3] J. D. Litster,[4] and Satyendra Kumar[5]
[1]*Department of Physics, Korea University, ChoongNam 339-800, Korea*
[2]*School of Applied and Engineering Physics, Cornell University, Ithaca, New York 14853*
[3]*Department of Physics, McGill University, Montreal, Canada H3A 2T8*
[4]*Department of Physics and Center for Materials Science and Engineering, Massachusetts Institute of Technology, Cambridge, Massachusetts 02139*
[5]*Department of Physics, Kent State University, Kent, Ohio 44242*
(Received 11 August 1997)

The nematic (N) to lamellar (L_α) phase transition in binary mixtures of cesium-perfluoro-octanoate (CsPFO) and water has been studied by high-resolution synchrotron x-ray scattering at 46.6 weight % CsPFO. The longitudinal correlation length $\xi_\parallel$ and the susceptibility σ associated with the lamellar phase fluctuations in the N phase, measured over three decades of reduced temperature, diverge with critical exponents $\nu_\parallel = 0.86 \pm 0.04$ and $\gamma = 1.37 \pm 0.11$, respectively. These results show that the N to L_α phase transition is quantitatively similar to the N to smectic-A phase transition of thermotropic liquid crystals with a wider nematic range. [S1063-651X(98)50804-5]

PACS number(s): 64.70.Md, 87.15.Da, 78.20.Fm, 82.60.Fa

The nematic (N) to smectic-A (A) phase transition is one of the most elusive problems in liquid crystal physics. At first glance, the N to A phase transition [1] appears to be a physical example of a one-dimensional melting/freezing transition. In the simplest case, one expects to find a second-order phase transition. However, existing theoretical models [2] disagree with high-precision experimental results on a large number of compounds whose nematic ranges vary [3] from just a few degrees to approximately 70°. The nematic range is an important measure of the coupling between the nematic order parameter and the smectic order parameter. The ratio T_{NA}/T_{NI}, of the N to A and N to isotropic phase transition temperatures, serves as a convenient but rough measure of the extent of this coupling. Increasing coupling (i.e., $T_{NA}/T_{NI} \rightarrow 1$) drives the N to A transition from second to first order. Another factor contributing to the richness of this phase transition is the Landau-Peierl's instability [4] in which the amplitude of the long-wavelength layer fluctuations diverges logarithmically with sample size. These fluctuations formally destroy the long range periodic order of the A phase.

Experimental studies of the N to A transition conducted over the past twenty years have focused on thermotropic liquid crystals. As extensively reviewed by Garland and Nounesis [5], thermotropic materials show the theoretically predicted [6] complex crossover from $3d$ XY to tricritical behavior. The anisotropic behavior expected from the coupling between the smectic order parameter and nematic fluctuations is also observed. These conclusions are based on high-precision results of over 30 studies of thermotropic liquid crystals. In contrast, lyotropic liquid crystals, which provide the opportunity to test the theoretical predictions and the independence of the critical behavior from chemical (microscopic) details, have only been tapped for a handful of experiments. This can be attributed, in large part, to the technical difficulties associated with handling these materials. The phase transition temperatures [7,8] are extremely sensitive to the concentration. Furthermore, good alignment of the director field, crucial for obtaining high-quality x-ray results, is difficult to achieve. Surface alignment does not penetrate into the bulk and magnetic alignment is frequently ineffective because the diamagnetic anisotropy of lyotropic materials [9] is typically two orders of magnitude smaller than in thermotropic materials.

We selected binary mixtures of cesium perfluorooctanoate, CsPFO, and H_2O for our study. CsPFO exhibits a micellar nematic phase N_D of disk-shaped micelles over a wide range of concentrations and the diamagnetic anisotropy of the micelles is positive [9]. The phase diagram of this system has been extensively studied and found to be isomorphous to thermotropic materials. At a fixed concentration, the system exhibits an isotropic phase at high temperatures. As the temperature is lowered, the N_D phase appears. At still lower temperatures, the micelles arrange themselves into bilayers, forming the L_α phase.

The synthesis group of the Liquid Crystal Institute at Kent State University headed by M. Neubert provided the necessary high-purity CsPFO. The samples are prepared by dissolving 46.6 wt % CsPFO in distilled, deionized, and degassed water and stirring for two days. The samples are then sealed in a beryllium cell (2.5 mm×4.5 mm×23 mm) to prevent H_2O evaporation and the resulting drift of transition temperatures. They are aligned by heating to the isotropic (I) phase and cooling slowly into the N_D phase in a ~ 7 kG magnetic field produced by a pair of samarium-cobalt permanent magnets and concentrated to a small volume by an iron yoke and tapered poles. The sample temperature is controlled with a long term stability of ± 1 mK. The sample chamber is thermally insulated from the surroundings. Beryllium x-ray windows on the chamber eliminate any temperature gradients in the sample due to air convection.

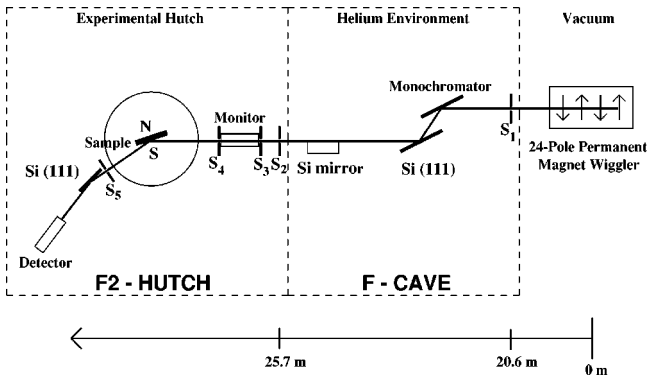

FIG. 1. Scattering geometry of the F-2 beam line at CHESS.

The high concentration of Cs and F in the samples strongly attenuates conventional Cu $K\alpha$ radiation. We circumvent this difficulty by using beam line F-2 at the Cornell High Energy Synchrotron Source (CHESS) and performing our measurements using 20.0 keV x rays ($\lambda = 0.620$ Å). The experimental setup is shown schematically in Fig. 1. A double bounce Si(111) monochromator selects a particular wavelength of the white radiation spectrum produced by the 24-pole permanent magnet wiggler. An ionization chamber monitors the intensity of the monochromatic beam incident on the sample. Two pairs of tantalum xy slits, S_3 and S_4, define the illuminated sample volume. A perfect Si(111) crystal serves as an analyzer and the x rays are detected by a Na(Tl)I scintillation detector.

The resolution in the scattering plane is determined by the Darwin widths of the monochromator and analyzer crystals, the angular divergence and source size of the white x-ray beam. In practice, at the small $\mathbf{q}$ values of interest for this experiment, the transverse component of the resolution function is nearly two orders of magnitude smaller than the longitudinal component. The resolution function $R(\mathbf{q})$ is measured by performing a 2θ scan of the main beam. This scan is accurately modeled by a sum of three Lorentzians (see Fig. 2). Consequently, the longitudinal and transverse components (full width at half maximum) of the resolution function are determined to be 2.6×10^{-4} Å^{-1} and 1.6×10^{-6} Å^{-1}, respectively. The component of the resolution perpendicular to the scattering plane is determined by the slits. This component of the resolution function, measured by rocking a silicon crystal in the sample position, is 5.6×10^{-3} Å^{-1}.

When studying thermotropic liquid crystals, one typically measures the temperature dependence of the critical scattering by performing both longitudinal and transverse scans through the peak in the scattering due to the smectic density wave while lowering the sample temperature through the N phase and approaching the A phase. This is not possible in the CsPFO system. The large rotations ($\pm 30°$) of the sample cell required to perform the transverse scans cause the transverse line shape and peak position to vary unpredictably with every scan. We find this to be due to fluid flow in the sample cell destroying the alignment obtained by cooling the sample from the I phase in the magnetic field. Consequently, we are limited to performing transverse scans only very close to T_c where the sample becomes more viscous and where the peak widths become narrower, requiring smaller angular rotations.

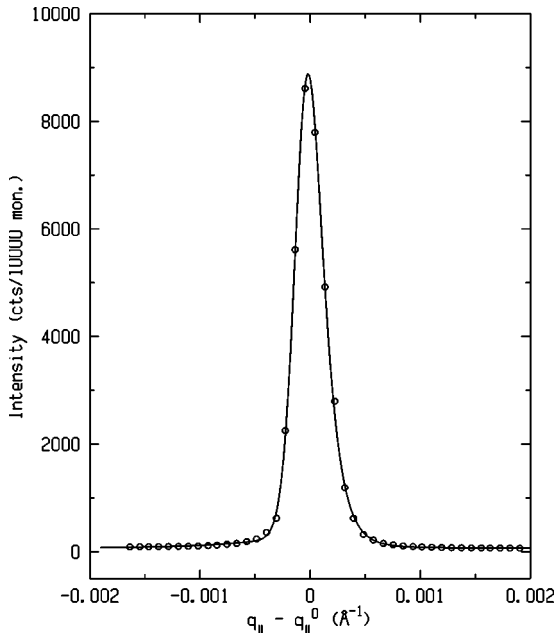

FIG. 2. Arm-zero profile. The solid line is the best fit to a sum of three Lorentzians. Full width at half-maximum is 2.6×10^{-4} Å^{-1}.

In contrast, longitudinal scans, which only require small rotations ($\pm 0.1°$) of the sample cell, are performed over three decades of reduced temperature, $t(=T/T_{NL_\alpha}-1)$.

A scan on the empty beryllium sample cell (Fig. 3) is used to measure the q dependence of the background. It has two components: the first is due to the proximity of the incident beam and gently slopes away from $q=0$; the second is due to the beryllium windows and has a peak at q_{bg} ~ 0.433 Å^{-1}. The measured background is accurately described by the sum of a second-order polynomial and a Lorentzian,

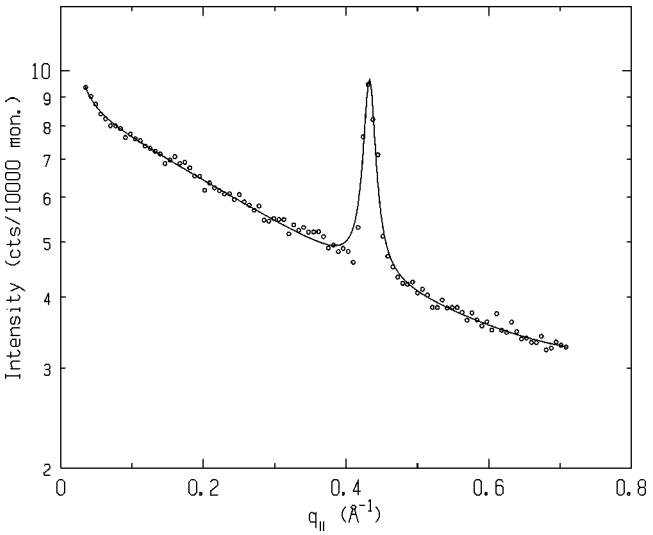

FIG. 3. Longitudinal scan of the empty beryllium cell yields the angular dependence of the background consisting of a well-defined peak due to the beryllium cell and upstream windows. The solid line is the best fit to Eq. (1). The beryllium peak is positioned at 0.433 Å and has FWHM$=8.7\times10^{-3}$ Å.

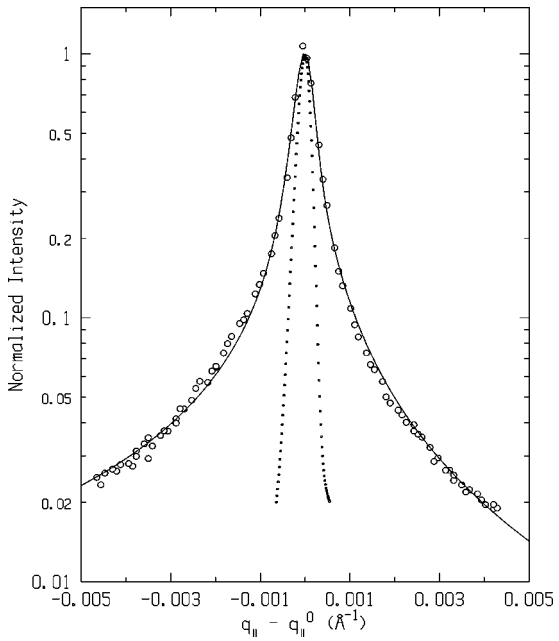

FIG. 4. Scattered x-ray intensity near the lamellar layer spacing peak. The circles represent the measured longitudinal scan at $t = 1.95\times10^{-5}$. The solid line is the best fit to Eq. (3) with the modified resolution function. The dotted line is the measured resolution function.

$$B(q) = c_0 + c_1 q + c_2 q^2 + \frac{A_0}{1 + B_0 (q - q_{\mathrm{bg}})^2}, \qquad (1)$$

and the best fit is shown as the solid line in Fig. 3.

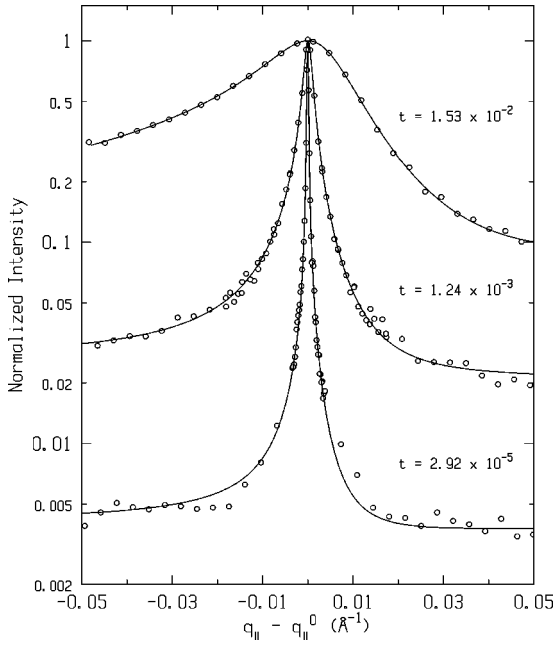

FIG. 5. Representative longitudinal scans at $t = 2.92\times10^{-5}$, 1.24×10^{-3}, and 1.53×10^{-2}. The solid lines are the best fits to Eq. (3). The values of scattering vector and $\xi_\parallel$ for the three scans are 0.1278 Å^{-1}, 24 300 Å; 0.1287 Å^{-1}, 1140 Å; and 0.1327 Å^{-1}, 117 Å, respectively. Approximate ratio of intensities at the three temperatures are 100:20:1, respectively.

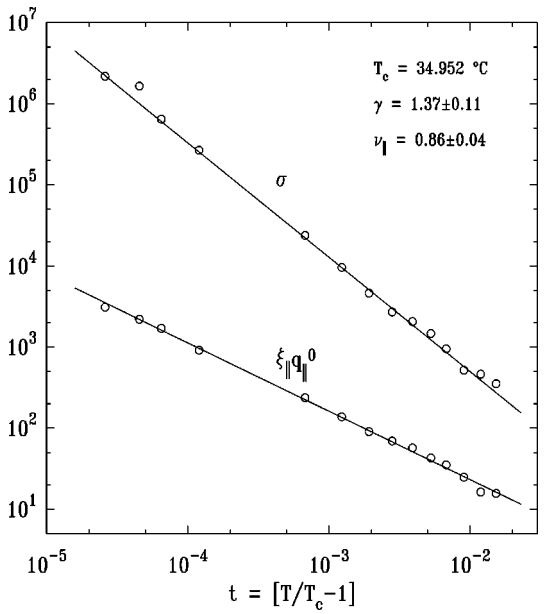

FIG. 6. Temperature dependence of the parallel correlation length $\xi_\parallel$ and smectic susceptibility σ near the critical temperature. The solid lines are the best fits to a single power with T_c fixed at the average of the value obtained from individual fits to the two quantities.

We analyze the x-ray scattering data by assuming that the static structure factor is given by the modified Ornstein-Zernike structure factor proposed by Als-Nielsen [10],

$$\mathcal{S}(\mathbf{q}) = \frac{\sigma}{1 + \xi_\parallel^2 (q_\parallel - q_\parallel^0)^2 + \xi_\perp^2 q_\perp^2 (1 + c\xi_\perp^2 q_\perp^2)}. \qquad (2)$$

Here, $\xi_\parallel$ and $\xi_\perp$ are the longitudinal and transverse correlation lengths, and σ is the smectic susceptibility. The additional $q_\perp^4$ term in the denominator is empirical and has previously been found necessary [11] to describe the data accurately. Empirically, the layer spacing is found to be weakly temperature dependent, with $q_\parallel^0 (= 2\pi/d)$ ranging from 0.1254 Å^{-1} to 0.1327 Å^{-1} for the particular mixture under study.

The micellar form factor is assumed to be given by the Bessel function of order zero, $J_0(aq)$. This is equivalent to assuming that the disk-shaped micelles have a circular cross section of radius a and constant density. While this is clearly a gross approximation, $J_0(aq)$ is a simple mathematical function that accurately describes the observed scattering and requires only one adjustable parameter.

The scattered intensity is then given by the sum of the background and the convolution of the resolution function with the product of the square of the micellar form factor and the static structure factor,

$$I(q) \sim B(q) + \int_{-\infty}^{\infty} dk\, R(q-k) |J_0(aq)|^2 \mathcal{S}(q). \qquad (3)$$

However, fits to Eq. (3) are not acceptable. The quality of the fits improves dramatically when a mosaic correction is included in the resolution function. The transverse scans performed near T_{NL_α} are used to monitor the sample mosaic. Empirically, the sample mosaic and the effect of changing

$\xi_\perp$ is accurately described by a Gaussian with a temperature dependent width. Using Eq. (3) with the measured sample mosaic incorporated into the resolution function, we were able to accurately model the line shape of the scattered intensity. A typical scan, taken at $t=1.95\times10^{-5}$, the modified resolution function, and the best fit to Eq. (3), are shown in Fig. 4.

Figure 5 shows representative longitudinal scans through the lamellar peak at three different reduced temperatures, t: 2.92×10^{-5}, 1.24×10^{-3}, and 1.53×10^{-2}. The dramatic changes in both the line width and the peak intensity are clearly evident. The solid lines are the best fits to Eq. (3). The divergent critical behavior of the parallel correlation length and smectic susceptibilty is depicted in Fig. 6 in which a dimensionless number $\xi_\parallel q_0$ and σ have been plotted as functions of reduced temperature. The solid lines are fits to single power laws of the forms $\sigma=\sigma_0 t^{-\gamma}$ and $\xi_\parallel=\xi_\parallel^0 t^{-\nu_\parallel}$. The best fit values are $\gamma=1.37\pm0.11$, and $\nu_\parallel=0.86\pm0.04$ where the uncertainties are obtained by using temperature range shrinking.

The values of T_{NL_α} obtained from the fits to $\nu_\parallel$ and γ are 34.950 and 34.954 °C, respectively, when transition temperature is treated as an adjustable parameter. The difference in the best fit values of $\nu_\parallel$ and γ produced by the 4 mK difference in T_{NL_α} is negligible. The average value of $T_{NL_\alpha}=34.952$ °C is very close to the value obtained by observing the sample mosaic.

The resolution function, the micellar form factor, and the mosaicity correction are all required to obtain high-quality fits of the scattered intensity. In contrast, fixing c, the coefficient of the fourth-order term in Eq. (2), to zero does not significantly change the quality of the fits. However, the best fit value of c does increase with increasing reduced temperature. Similarly, the micellar form factor has a large effect at large values of the reduced temperature. It is quantitatively important for $t>5.0\times10^{-4}$. On the other hand, the mosaicity correction is important only near T_{NL_α} as the linewidth approaches the resolution limit.

In summary, we have measured the critical behavior of the lamellar layer fluctuations in the nematic phase of a lyotropic liquid crystal with $T_{NL_\alpha}/T_{NI}=0.98$. Our results show that the values of $\xi_\parallel$ and σ exhibit single power law divergences with exponents 0.86 ± 0.04 and 1.37 ± 0.11, respectively. The value of the exponent $\nu_\parallel$ is not equal to the $3d$-XY model value. Although we are not able to measure $\nu_\perp$, there is ample evidence that these materials also exhibit anisotropic divergence as in the case of thermotropic liquid crystals. Using the hyperscaling relation, $\nu_\parallel+2\nu_\perp=2-\alpha$, a value of $\nu_\perp\cong0.57$ is expected. Here, $\alpha\sim0$ is the heat capacity exponent [7]. From the dependence [5] of $\xi_\parallel$, $\nu_\perp$, γ, and α on T_{NA}/T_{NI}, it is clear that within acceptable errors, this system behaves like a thermotropic liquid crystal with a lower value of $T_{NA}/T_{NI}\sim0.92$.

[1] W. L. McMillan, Phys. Rev. A **4**, 1238 (1971); **6**, 936 (1972); K. K. Kobayashi, J. Phys. Soc. Jpn. **29**, 101 (1970); W. L. McMillan, Phys. Rev. A **4**, 1238 (1971); P. G. de Gennes, Solid State Commun. **10**, 753 (1972); T. C. Lubensky, J. Chem. Phys. **80**, 31 (1983).

[2] T. C. Lubensky and A. J. McKane, J. Phys. (France) Lett. **43**, L-217 (1982); W. Helfrich, J. Phys. (Paris) **39**, 1199 (1978); D. R. Nelson and J. Toner, Phys. Rev. B **24**, 363 (1981); C. Dasgupta and B. I. Halperin, Phys. Rev. Lett. **47**, 1556 (1981).

[3] L. Chen, J. D. Brock, J. Huang, and S. Kumar, Phys. Rev. Lett. **67**, 2037 (1991); B. M. Ocko, R. J. Birgeneau, and J. D. Litster, Z. Phys. B **62**, 487 (1987), and references therein.

[4] J. Als-Nielsen, J. D. Litster, R. J. Birgeneau, M. Kaplan, C. R. Safinya, A. Lindegaard-Anderson, and S. Mathiesen, Phys. Rev. B **22**, 312 (1980).

[5] C. W. Garland and G. Nounesis, Phys. Rev. E **49**, 2964 (1994).

[6] B. R. Patton and B. S. Andereck, Phys. Rev. Lett. **69**, 1556 (1992), and references therein.

[7] S. S. Shin, S. S. Keast, M. E. Neubert, D. Finotello, and S. Kumar, Phys. Rev. A **45**, 8683 (1992).

[8] T. Haven, D. Armitage, and A. Saupe, J. Chem. Phys. **75**, 352 (1981).

[9] N. Boden and M. C. Holmes, Chem. Phys. Lett. **109**, 76 (1984); N. Boden, P. H. Jackson, K. McMullen, and M. C. Holmes, *ibid.* **65**, 476 (1979); N. Boden, S. A. Corne, M. C. Holmes, P. H. Jackson, D. Parker, and K. W. Jolly, J. Phys. (Paris) **47**, 2135 (1986).

[10] J. Als-Nielsen and R. J. Birgeneau, Am. J. Phys. **45**, 554 (1977).

[11] J. Als-Nielsen, R. J. Birgeneau, M. Kaplan, J. D. Litster, and C. R. Safinya, Phys. Rev. Lett. **39**, 352 (1977).